# THE GEOLOGY OF THE OCEANOGRAPHER TRANSFORM: THE TRANSFORM DOMAIN

OTTER Team

(Oceanographer Transform Tectonic Exploration and Research Team)

P. J. FOX[1], R. H. MOODY[2], J. A. KARSON[3], E. BONATTI[4], W. S. F. KIDD[2], K. CRANE[4], D. G. GALLO[1], J. B. STROUP[2], D. J. FORNARI[4], D. ELTHON[5] P. HAMLYN[4], J. F. CASEY[5], D. NEEDHAM[6], and R. SARTORI[7]

(Accepted 12 May, 1985)

**Abstract.** Three dives in submersible ALVIN and four deep-towed camera lowerings have been made along the transform valley of the Oceanographer Transform. These data constrain our understanding of the processes that create and shape the distinctive morphology that is characteristic of slowly slipping ridge-transform-ridge (RTR) plate boundaries. Our data suggest that the locus of strike-slip tectonism, called the transform fault zone (TFZ), is confined to a narrow swath (<4 km) that is centered along the axis of maximum depth. The TFZ is flanked by the inward facing slopes of the transform valley. The lower portions of the valley walls are characterized by broad sloping exposures of undisrupted sediment but at higher elevations the walls are made up of inward facing scarps and terraces of variable dimensions. Although the scarps have been badly degraded by mass wasting, there is no evidence to suggest that these scarps have accommodated significant amounts of strike-slip motion. Plutonic and ultramafic rocks are exposed on these scarps and the occurrence of this diverse assemblage on small-throw faults indicates that the crust is thin and/or discontinuous in this environment. We suggest that this complex igneous assemblage is the product of anomalous accretionary processes that are characteristic of slowly-slipping RTR plate boundaries.

## 1. Introduction

Slowly slipping RTR plate boundaries are common occurrences along the Mid-Atlantic Ridge (MAR) south of the Azores (e.g., Heezen and Tharp, 1968; Phillips and Fleming, 1978). These plate boundaries are characterized by anomalously deep, elongate troughs that abruptly truncate ridge axis parallel terrain and that develop thousands of meters of relief (e.g., Heezen *et al.*, 1964). Kinematic models of plate tectonics mandate that strike-slip relative motion must characterize the RTR environment (Wilson, 1965; Sykes, 1967) and, for the transform faults of the central North Atlantic that offset the MAR, reconstructions of magnetic anomaly results indicate that time-averaged slip-rates should be on the order of 20 mm to 30 mm $yr^{-1}$ (e.g., Pitman and Talwani, 1972). The detailed structural fabric of

[1] Graduate School of Oceanography, Univ. of Rhode Island, Narragansett, RI 02882, U.S.A.
[2] Dept. of Geological Sci., SUNY at Albany, Albany, NY 12222, U.S.A.
[3] Woods Hole Oceanographic Institution, Woods Hole, MA 02443, U.S.A.
[4] Lamont-Doherty Geological Observatory, Palisades, NY 10964, U.S.A.
[5] Dept. of Geology, Univ. of Houston, Houston, TX 77004, U.S.A.
[6] C.O.B., Boite Postale 337 29273, Brest Cedex, France.
[7] IGM/CNR, Via Zamboni 65, Bologna, Italy.

*Marine Geophysical Researches* **7** (1985) 329–358. 0025–3235/85.15

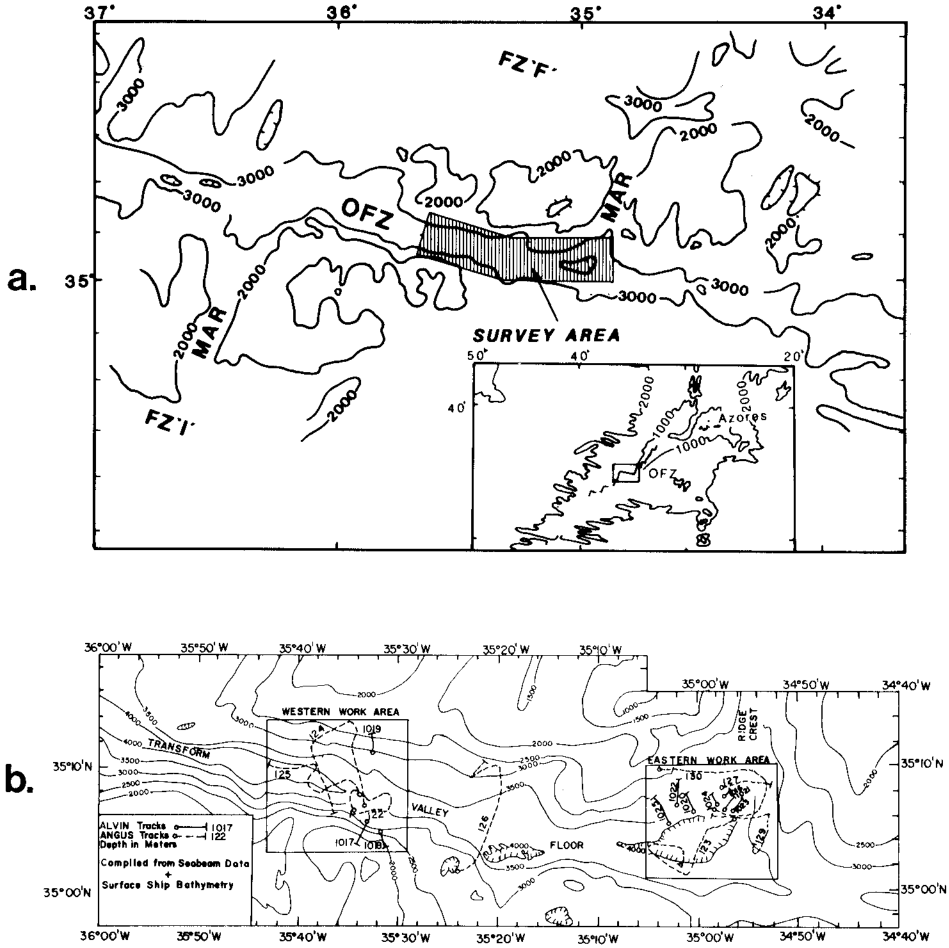


Fig. 1. (a) Generalized bathymetric map of a portion of the Oceanographer Fracture Zone (OFZ) including the transform. The adjoining ridge axes of the Mid-Atlantic Ridge (MAR) are shown as well; two small-offset fracture zones (FZ) are indicated at the limits of the map. The area investigated within the transform during our survey is shaded; small index map of northeastern Atlantic locating the OFZ is shown at lower right. Depth in meters; contour interval 1000 m. (b) Map of that portion of the Oceanographer Transform investigated during our ALVIN and ANGUS field program. The results from the eastern work area have been reported earlier (OTTER, 1984) and this paper presents the results for the western work area as well as ANGUS traverse 126. Depth in meters; contour interval 500 m.

RTR plate boundaries in the North Atlantic has gone largely unresolved because there has been a lack of high-resolution data at an appropriate scale. Deep-Tow (Detrick *et al.*, 1973) and in situ (ARCYANA, 1975; Choukroune *et al.*, 1978) investigations of the 20 km offset Transform A located at 37° N demonstrate that along this transform boundary evidence for recent tectonism is confined to a narrow belt less than two kilometers wide and is centered along the axis of maximum depth. Little was known, however, about the structural elements that characterize a large-offset (100 km) slowly slipping RTR plate boundary.

In the summer of 1980 an investigation of the Oceanographer Transform (OT; 35° N, 35° W) was conducted using the ANGUS deep-towed camera system and the manned submersible ALVIN (Figure 1a). Part of the field experiment was located at the eastern intersection of the OT with the axis of the MAR (Figure 1b) and the focus of this portion of the field program was to define the structural styles and outcrop relationships developed at and proximal to a ridge-transform intersection. These results have alrady been published (OTTER, 1984) and will not be dealt with in this paper. The other portion of the field program was located along the central portion of the transform and was designed to establish the vertical and lateral distribution of rock types exposed along the walls of the transform valley and to define the structural provinces that are characteristic of a large-offset slowly slipping RTR plate boundary.

## 2. Regional Morphotectonic and Geologic Properties of the Oceanographer Transform

The first-order morphotectonic properties of the OT, as defined by conventional surface-ship bathymetry, is described in detail in other publications (Fox *et al.*, 1969; Schroeder, 1977; Williams *et al.*, 1984; Fox *et al.*, in prep.) but is briefly reviewed here in order to put our detailed observations in a regional framework. The OT at 35° N offsets the axis of the MAR 130 km in a dextral sense along a WNW–ESE trending trough that can be best described as a broad, open, and V-shaped valley developing over 2000 m of relief. The transform valley walls intersect to create an axis of maximum depth that varies from 3700 to 4500 m along the length of the transform. The lower portions of the valley walls exhibit a strong transform-parallel grain but at shallower levels this transform-parallel fabric is frequently disrupted by small ridges and valleys with trends that are approximately ridge axis parallel (Figure 1b).

The southern flank of the transform valley, as outlined by the 2000 m contour, is defined by an E–W trending ridge that is approximately 10 to 20 km wide. This transverse ridge, however, is not continuous along the length of the south flank of the transform valley and its along-strike continuity is disrupted by N–S striking embayments. From the crest of this ridge the sea floor slopes steeply down towards the axis of the transform valley developing regional slopes of 10° to 20°. It is from numerous localities along the south wall of the transform valley that a diverse suit of basaltic, gabbroic and ultramafic rocks has been recovered (Shibata and Fox, 1975; Fox *et al.*, 1976). In contrast to the southern side of the transform valley, the northern flank does not develop a transverse ridge and is characterized by a number of N–S trending ridges and valleys that slope down into the transform trough developing regional gradients of 10° to 15°.

## 3. The Transform Valley: Near Bottom Observations

Three submersible traverses and four deep-towed camera traverses were carried out along the transform valley and, except for one ANGUS lowering, all of the near bottom traverses are located in one small area positioned along the center of the transform (Figures 1b, 2). The remaining ANGUS traverse (126), a N–S profile across the transform valley, is positioned about 20 km to the east of this work area (Figures 1b, 3). A synthesis of these observational data reveal that the transform valley can be divided into two morphotectonic provinces. The first province, a zone of tectonism, is a belt of terrain that is less than 4 km wide, that is centered about the axis of maximum depth, that is characterized by irregular topography, and that includes terrain disturbed by recent faulting. The second province is

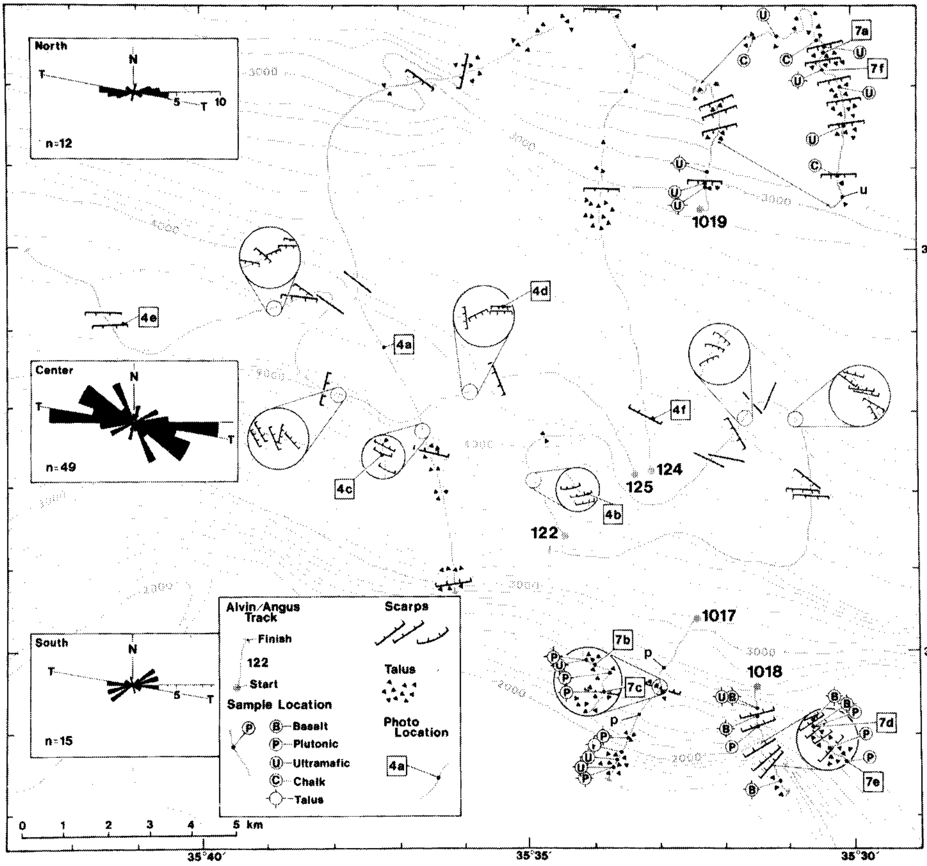


Fig. 2. Bathymetric map of the western work area (see Fig. 1b for location) showing the locations of the ANGUS and ALVIN traverses and the geologic relationships documented to exist along each traverse. Rose diagrams to the left of the field area summarize the structural orientation data for the north wall, transform valley floor and south wall and include data from ANGUS traverse 126. Depth in meters; contour interval 100 m.

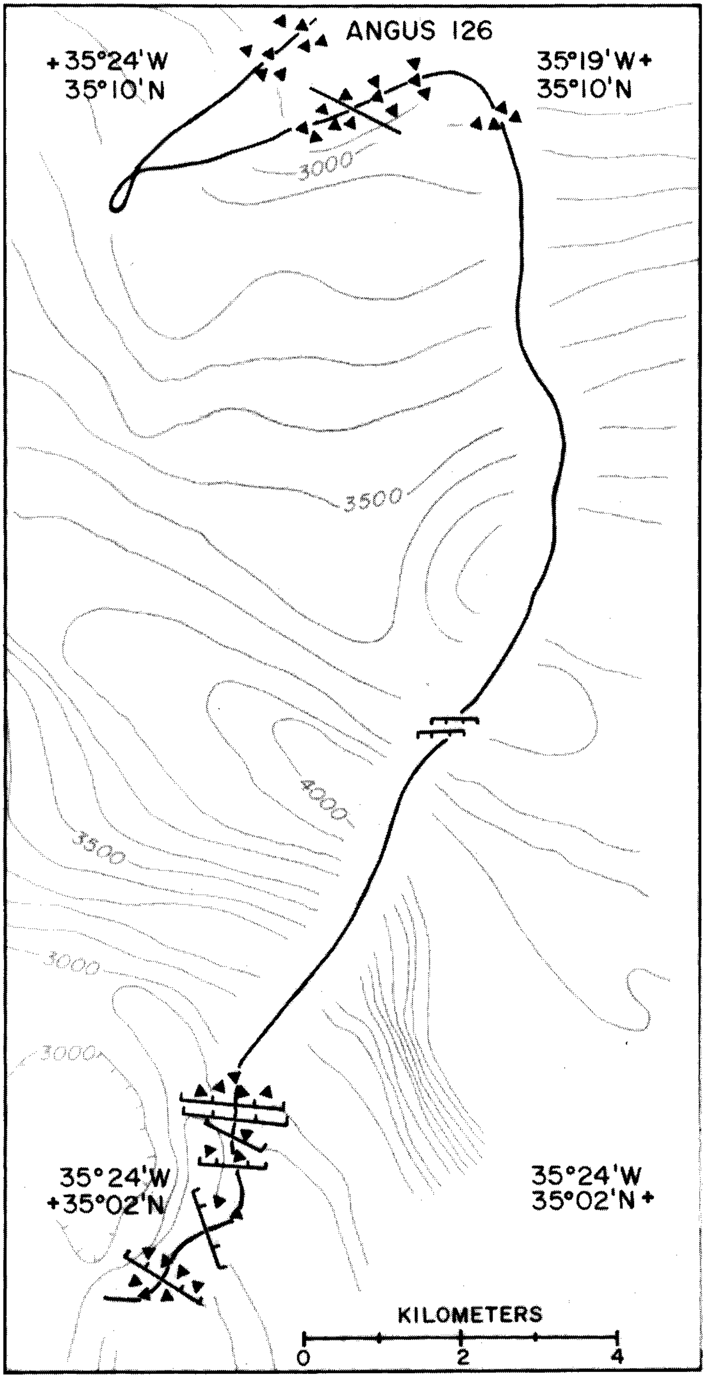


Fig. 3. ANGUS traverse 126 across the transform valley; see Figure 1b for location and Figure 2 for a key to the symbols used. Depth in meters; contour interval 100 m.

composed of the transform valley walls that flank the zone of neotectonism and that slope up and away from this zone over distances of several tens of kilometers. The transform valley walls exhibit no evidence for recent tectonism and slope morphology is presently controlled by sedimentation and slope decay.

### 3.1. The Axis of Maximum Depth: A Zone of Tectonism

Almost all of ANGUS camera lowerings 122 and 125 and portions of 124 and 126 traverse along or across the tectonized zone providing approximately 60 km of photographic data for this interval (Figures 2, 3). Most of these results are concentrated along a 20 km long portion of the axis and it is clear from these data that the fine-scale morphotectonic character of the terrain immediately flanking the axis of maximum depth is defined by variable and complexly arranged sedimented terrain. Surprisingly, not one outcrop and hardly any talus fragments of the igneous rock are observed along any of the ANGUS profiles; instead the sea floor is composed of a relatively smooth sediment interface that is undisrupted for many kilometers (Figure 4a). The seafloor immediately flanking the axis of maximum depth exhibits a gentle 10° slope. Superimposed upon this regional slope are ridges and troughs with relief of a few meters to several meters that create a hummocky outline in profile. The two-dimensional nature of the photographic profiles does not define the shape or orientation of these undulating terrain elements and it is difficult to determine whether or not these objects are arranged systematically creating a distinctive grain to the microtopography along the axis of maximum depth. The smooth sediment surface, however, that characterizes long portions of the seafloor in this environment is frequently punctuated by narrow intervals of rough, disrupted and heterogenous terrain elements that exhibit evidence for rapid changes in slope gradient and orientation. Moreover, evidence for slope modification in the form of fault scarps and/or active areas of mass wasting are observed as well (Figures 2, 3, 4b–f) and these areas are characterized by one or a number of closely spaced fault scarps that develop relief of several centimeters to a few meters exposing semiconsolidated carbonate (Figure 4b–f). A range of ages for these scarps is suggested because in some cases the scarp faces are free of any suggestion of bioturbidation and the base of these faults are devoid of debris (Figure 4b, c). At other localities small wedges of debris, in various stages of development, accumulate along the base of faults and fault traces are badly degraded by erosion, exhibiting a rounded rather than angular profile (Figure 4d, f). Steep unstable slopes with relief of a few meters to at least several meters are also observed at several locations (Figure 4e). The faces of these slopes are incised by erosional rills, and well developed debris deposits blanket the sea floor downslope from these steep sections.

These disturbed intervals are generally narrow and range from a few meters to several hundred meters in width. The limited perspective provided by the photographic cross sections makes it difficult to establish for certain the continuity of any given fault trace or composite of fault traces along strike, but the relatively

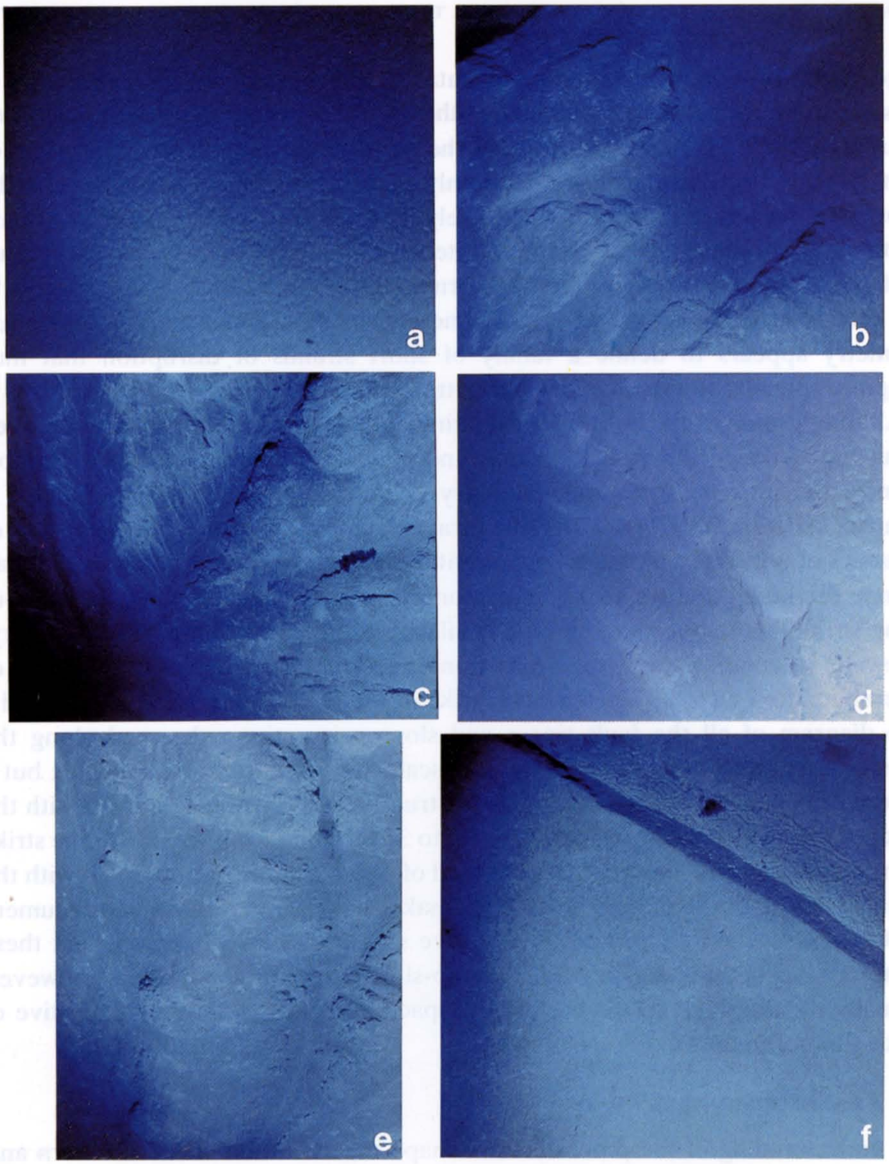


Fig. 4. Photographs of the floor of the transform valley; see Figure 2 for locations. (A) A typical photograph along the floor of transform – smooth undisrupted carbonate terrain (ANGUS photo; lowering 124; time 02:10:00; depth 4220 m). (B) A sequence of closely-spaced scarps several centimeters high that cut semiconsolidated carbonate (ANGUS photo, lowering 122; time 04:34:56; depth 3752 m). (C) A complex microtopographic environment where seafloor appears to plunge steeply to left; slope is cut by several closely-spaced erosional furrows and scarplets (ANGUS photo, lowering 124; time 04:38:42; depth 4103 m). (D) A sequence of badly degraded scarplets in semiconsolidated carbonate (ANGUS photo; lowering 125; time 01:20:50; depth 4130 m). (E) A steep slope that plunges steeply exposing bedded carbonate (ANGUS photo; lowering 125; time 11:23:08; depth 4160 m). (F) A relatively old, small scarp several centimeters high with a well-developed debris wedge at its base that shows considerable bioturbidation (ANGUS photo; lowering 124; time 15:41:35; depth 3680 m).

large concentration of photographic data in the primary work area makes it possible to assess with some confidence the spatial distribution of these disturbed intervals along a 20 km long portion of the axis of maximum depth. The zones of neotectonism do not seem to be randomly positioned along this segment of the transform, but rather these intervals closely flank (< 1.5 km) the axis of maximum depth and, in some cases, tectonized terrain can be extrapolated with some confidence along the strike of the transform axis from one closely spaced profile to the next over distances of several kilometers. In plan view, the apparent fault geometry appears to define a family of short strands of disruption that may integrate spatially to create a braided pattern (Figure 2).

Although some of the intervals of faulting and slope modification can be traced along the strike of the transform axis and appear to define a network of short strands, the internal structural geometry developed within a given interval is complex and variable (Figure 2). When traversing across a disturbed interval over distances of a few tens of meters the orientation and facing direction of scarps can change markedly and for those neotectonic zones that appear to be continuous along strike there appears to be little similarity with respect to internal geometry: the scale, orientation and facing direction of structures change over distances of several hundred meters. The regional strike of the OT is WNW–ESE (100°) and a rose diagram of all the fault traces and slope orientations observed along the transform axis demonstrates that the fine scale structural fabric is complex but a pattern does emerge with the majority of structures oriented sub-parallel with the strike of the axis of maximum depth or 20° to 30° oblique to either side of the strike of the transform axis (Figure 2). These kind of photographic data coupled with the unstable nature of the sedimented terrain makes it difficult to rigorously document fault kinematics and there are no definitive strain markers to suggest that these faults have accommodated anything but dip-slip motion. In several areas, however, mutually parallel fault traces are closely spaced creating a texture suggestive of strike-slip deformation (Figure 4b, c).

### 3.2. Transform Valley Walls

Our understanding of the processes that shape the evolution of the northern and southern walls of the OT are based on the analysis of data obtained during ALVIN dives (1017, 1018, 1019) and portions of three ANGUS lowerings (122, 124, 126). Dives 1017 and 1018 along with some photographic data from ANGUS 122, 124, and 126 are located along the south wall (Figures 2, 5, 7) while dive 1019 and portions of ANGUS lowerings 124 and 126 are located along the northern valley wall (Figures 2, 3, 5, 6).

The surface-ship wide-beam echo sounding data suggest that the transform walls slope, in a monotonous fashion, down towards the axis of maximum depth. This picture, however, represents only a first-order approximation and our traverse data indicate that the valley walls, both north and south, are composed of two principal terrain elements: terraces of variable width and scarps with variable relief. At lower elevations on the transform valley walls (3500 m to 2500 m), the terraces are broad (500 m to greater than 1000 m) and their continuity is only infrequently disrupted by scarps with modest relief (10 m or less). At higher elevations on the walls of the transform (depths <2500 m) the width of the terraces diminishes markedly (<500 m) and the frequency of scarps dramatically increases (Figures 5, 6). As a result of this systematic distribution, the spatial integration of the terraces and steep intervals create staircase-like profiles that are asymmetric in cross section: at lower elevations the terraces are broad and the rise between terraces is small but at higher elevations the terraces are very narrow and the cumulative relief of the numerous scarps is large.

The terrace surfaces are covered by a blanket of sediment of unknown thickness and dip gently (5° to 15°) down towards the valley axis. Apart from the evidence of extensive bioturbidation, the surfaces of these terraces are very smooth and are covered with a thin (<2 cm) veneer of pteropod shells mixed with fine-grained mocha-colored debris that is underlain by an off-white, coherent carbonate ooze. Only occasionally is the remarkable along the across-strike continuity of the terrace surfaces interrupted by isolated talus blocks that protrude through the sediment (Figure 7a). It appears that these exotic blocks must have been in place for a considerable length of time because they are uniformly covered with a coating of manganese, they often provide the foundation for sessile organisms, and the sea floor surrounding these blocks is often littered with sand-sized inorganic debris spalled from rock surfaces. Furthermore, there are no skid marks apparent in the sedimented surfaces upslope from the talus blocks to suggest a recent downslope migration.

The monotony of the terraces is punctuated by steep intervals made up of either scarps that expose the underlying basement rocks (Figure 7d–f) or precipitous sedimentary slopes (30° to 60°) composed of a chaotic admixture of talus and carbonate (Figure 7c). The infrequently encountered steep intervals at lower elevations (depths greater than 2500 m) on the transform walls exhibit relief of only a few to several meters and are not laterally continuous along strike for more than several tens to a few hundreds of meters. The outcropping of basement along these steep intervals is rare and scarps generally expose blocks of rock ranging from cobble-sized fragments to large bolsters that are set in a semiconsolidated matrix of fine-grained material (e.g., carbonate, inorganic sand). The faces of these steep intervals have been degraded by mass wasting and are often deeply incised by erosional gullies the axes of which are littered with gravel and sand-sized debris. In addition, well developed aprons of debris fan out from these outcroppings and stringers of dark inorganic material can be traced for tens of meters downslope from these exposures.

At higher elevations (depths <2500 m) on the transform valley walls the scarps are better developed and sections of semi-consolidated debris or bedrock (plutonic or ultramafic rocks) are frequently exposed on near vertical (>60°) slopes with relief of a meter or less to tens of meters. Like the smaller scarps observed at

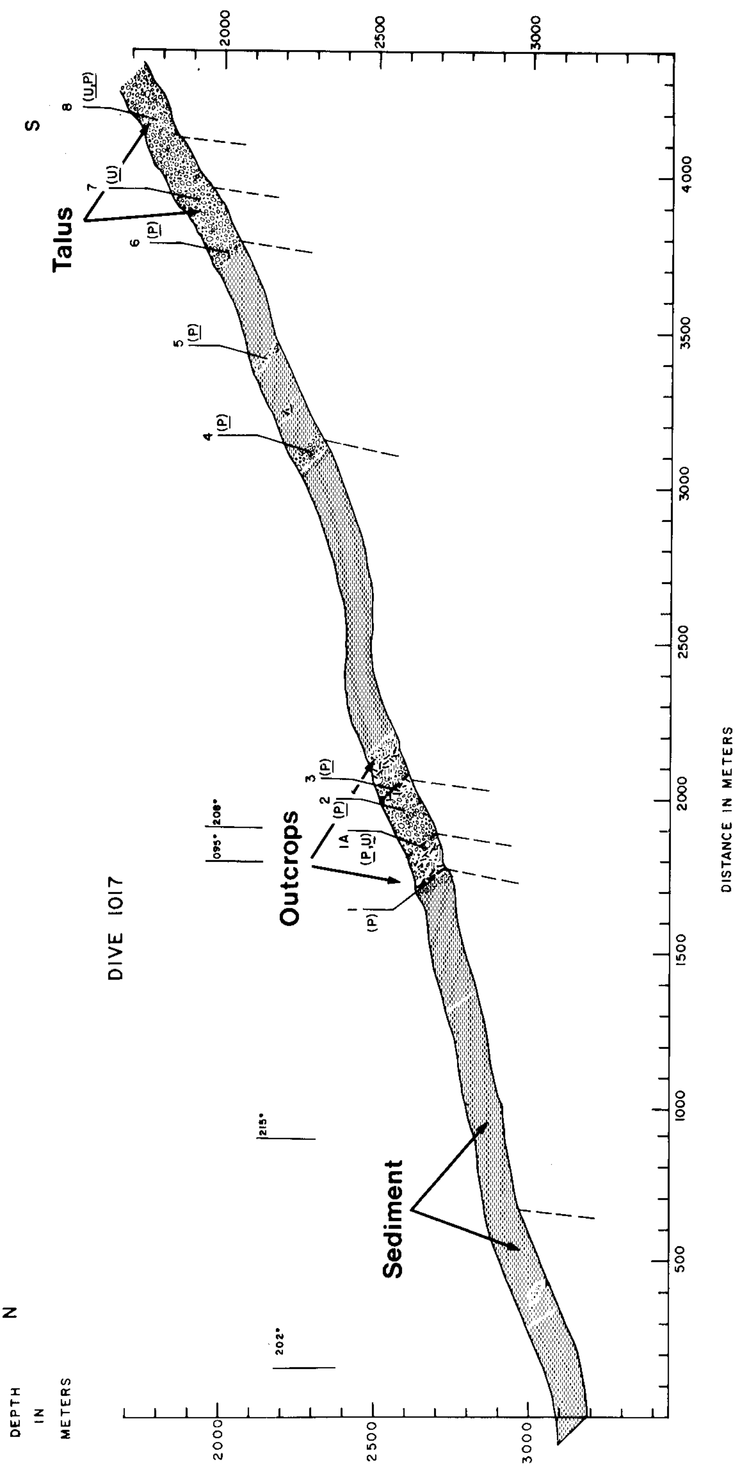
DIVE 1017
S
N
Talus
Outcrops
Sediment
DEPTH IN METERS
DISTANCE IN METERS
2000
2500
3000
500
1000
1500
2000
2500
3000
3500
4000
202°
215°
095°
208°

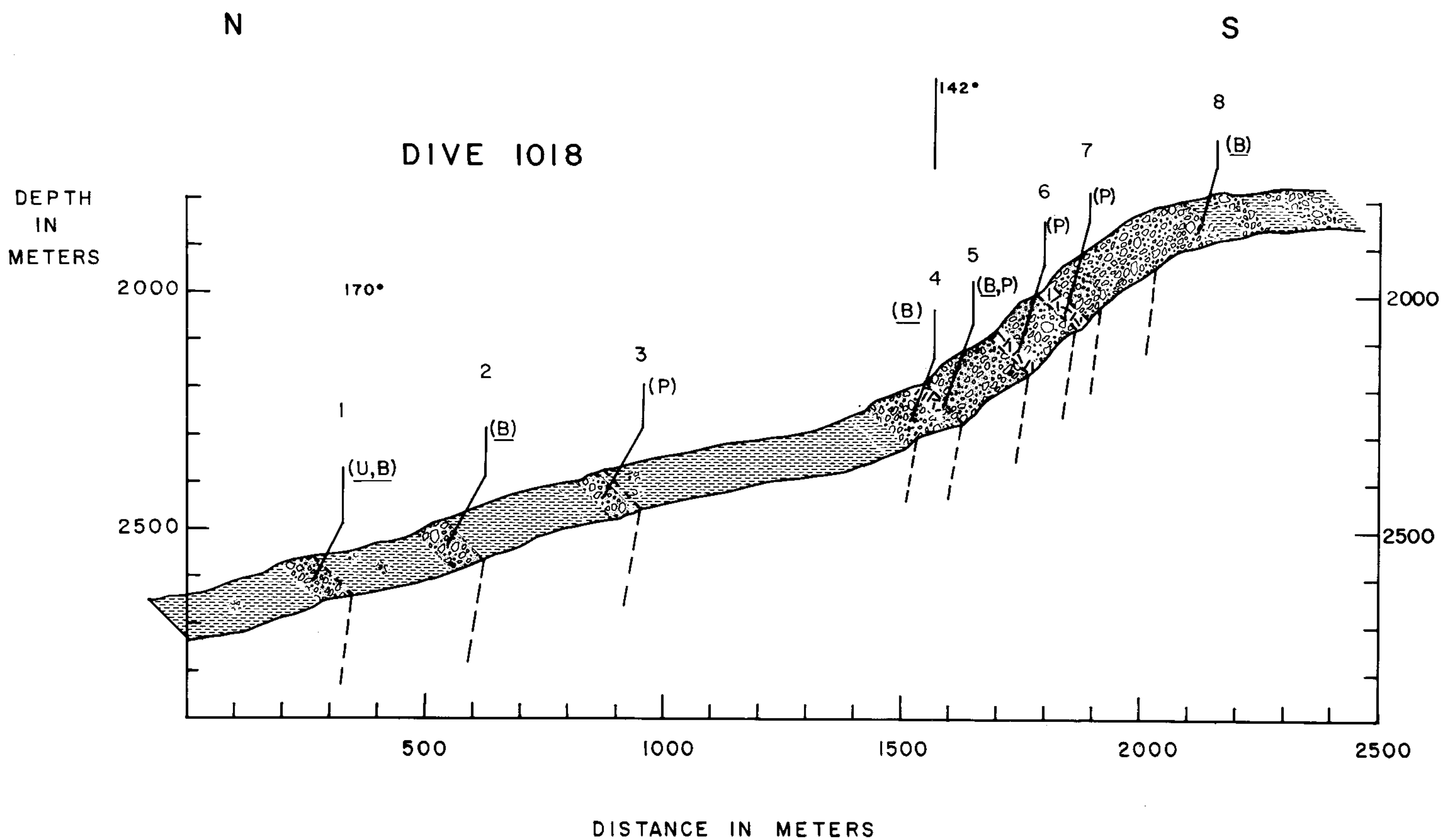


Fig. 5. Schematic geological cross-sections of ALVIN dives 1017 and 1018 (no vertical exaggeration). Letters B (basalt), P (plutonic) and U (ultramafic) indicate the locations and rock-type of samples collected along dive traverses; underlined letters indicate samples recovered from loose talus. Inferred fault scarps are indicated by dashed lines; fault dip is hypothetical. Vertical lines above section show course changes.

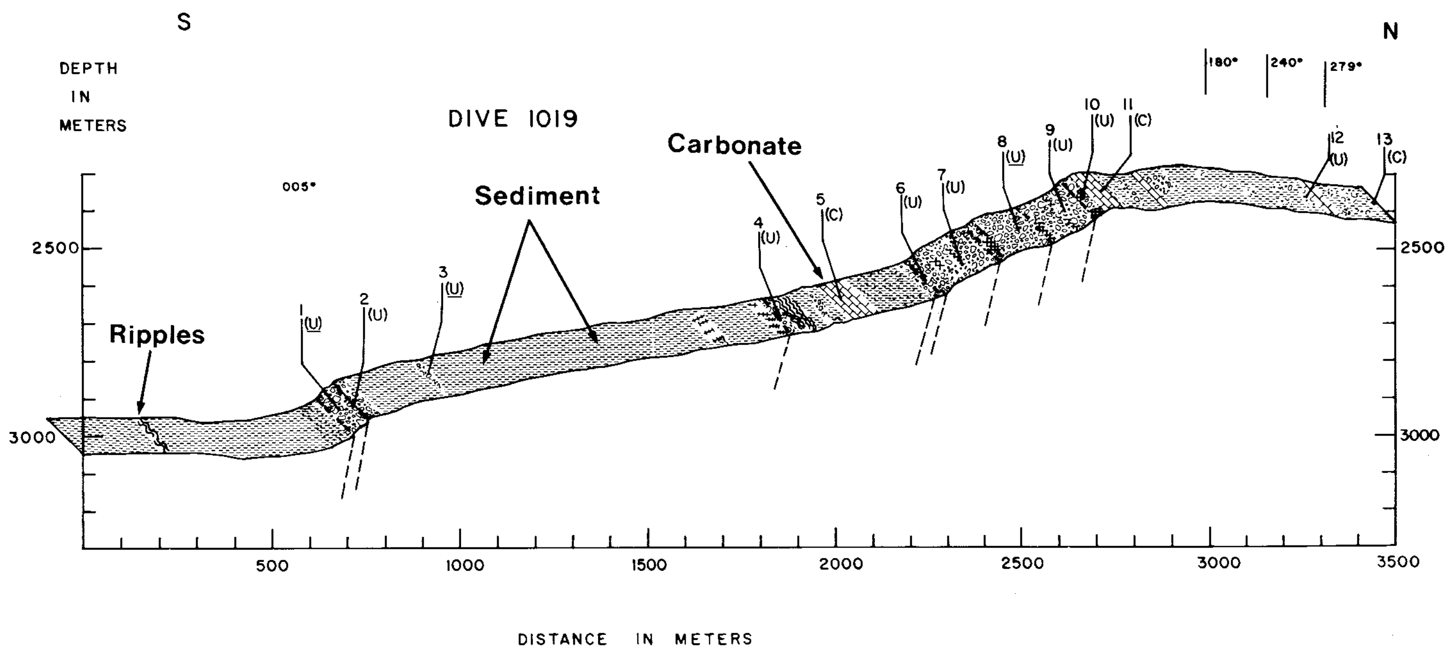


Fig. 6. Schematic geological cross-section of ALVIN dive 1019 (no vertical exaggeration). Letters C (semi-consolidated carbonate), and U (ultramafic) indicate locations and rock-type of samples collected along dive traverse; underlined letters indicate samples recovered from talus. Inferred fault scarps are indicated by dashed lines; fault dip is hypothetical. Vertical lines above section show course changes.

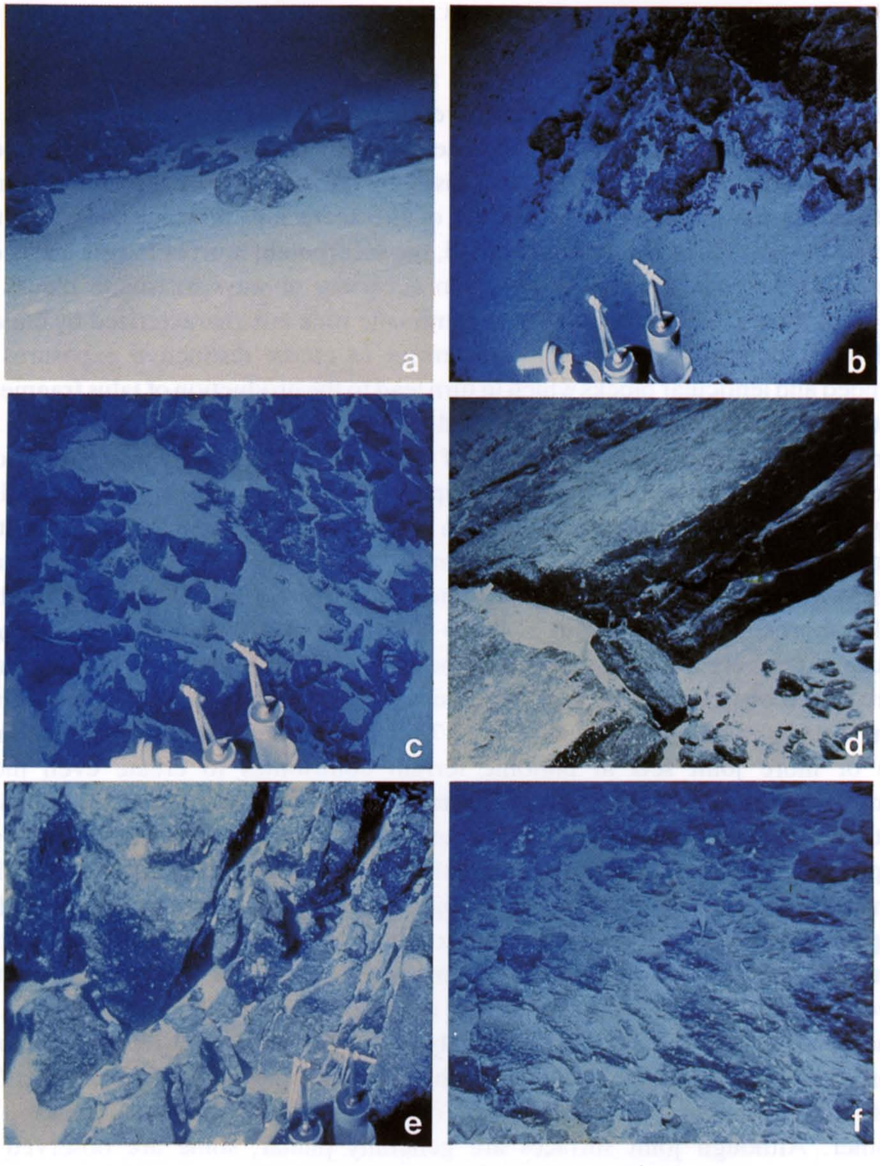


Fig. 7. ALVIN photographs of localities along the transform valley walls; see Figure 2 for locations. (A) Scattered talus blocks partially embedded in carbonate; sand-sized fragments of blocks litter area around blocks (ALVIN dive 1019; W. S. F. Kidd hand held photograph; depth 2425 m). (B) Steep escarpment exposing variably sized talus fragments set in a fine-grained matrix of carbonate and detrital grains (ALVIN dive 1017; hull-mounted camera; time 13:24:29; depth 2695 m). (C) Outcrop of plutonic rock cut by an anastomosing network of closely-spaced fractures (joints). Steep erosional chute can just be observed in lower right corner (ALVIN dive 1017; hull-mounted camera; time 14:31:22; depth 2601 m). (D) Outcrop of plutonic rock exhibiting very well defined joint pattern – moderately dipping (to north) surfaces that give the rock a tabular shape and are cut by a near vertical, N–S trending surface (ALVIN dive 1018; J. Karson, hand held photograph; time 16:28:15; depth 2276 m). (E) Outcrop of plutonic rock cut by a series of closely-spaced, near vertical joints that strike NW–SE (ALVIN dive 1018; hull-mounted photograph; time 18:20:00; depth 2032 m). (F) Degraded outcrop of ultramafic rock exhibiting a well-defined foliation that strikes at approximately 220° with a sub-vertical dip creating lozenge-shaped blocks (ALVIN dive 1019; W. S. F. Kidd hand held photograph; time 14:29:00; depth 2565 m).

localities lower on the transform walls, these scarps have all been modified by erosive processes. For distances of several tens of meters downslope from an escarpment the sea floor is littered with debris. Individual scarp faces, independent of the material exposed, are deeply incised by narrow, steeply dipping channels that disrupt the along-strike continuity of the scarp and that cut back into the transform wall. When bedrock is exposed, the escarpment morphology is markedly controlled by joint sets that intersect in a variety of ways to isolate blocks of different shapes. The outcroppings of ultramafic rock are characterized by curved and irregular parting surfaces that intersect to create distinctive exposures of rounded and lenticular blocks which in turn lead to the production of talus fragments that are distinctly oblate (well developed on Dives 1017, 1019; Figure 7f).

In contrast to the rounded exposures of ultramafic rock, the integrity of outcrops composed of plutonic rock is often disrupted by one or more sets of planar joints (Figure 7d–e) that produce outcrops with angular facets. At a number of localities along the south wall many of the plutonic rock outcrops are defined by planar transform-parallel faces that are disrupted by a closely-spaced joint set with a strike approximately E–W and a dip to the north of 40° to 60°. Large tabular blocks of talus are found at the base of these plutonic rock outcrops and thin slabs of rock are observed to be separating away from these escarpment faces along joint surfaces parallel to the face (Figure 7d). At other localities the intersection of two or more joint sets in plutonic terrain contributes to create even more complexly shaped outcrop patterns and talus blocks. At some outcrops, joint sets that strike approximately N–S and that exhibit a variety of dips (vertical, steeply dipping to either the E or W) along with the frequently observed E–W striking joint systems intersect to produce triangular promontories (Figure 7e). Oddly-shaped rhombohedral, rectangular and triangular shaped blocks of plutonic rock found as talus at the base of escarpments attest to the importance of the development of these joint systems in the control of scarp evolution (Figure 7c). In general terms, the joint systems are variable and spatially heterogeneous with joint character, distribution, and orientation changing radically over a distance of a few tens of meters across one escarpment or from one closely spaced outcrop to another. Although joint surfaces are generally planar, some are observed to anastomose and outline blocks of various dimensions (Figure 7c, e).

The escarpments observed along the north and south walls of the transform valley are notable in that they all face the transform axis, individually they generate relief of no more than a few tens of meters, they are best developed at localities positioned high on the valley walls, and their recent history has been determined by the processes associated with slope decay and not slope generation. In fact, there is no evidence along any of the towed camera or submersible traverses to suggest that recent and on going faulting is important in shaping the morphology of these portions of the transform valley walls. The rock outcrops are all painted with a veneer of Mn and are often covered with sessile organisms. Sediments are observed to abut, in an undisrupted fashion, against the foot of the rock escarpments indicating that there has been little or no recent relative motion. Furthermore, the smooth sedimented surfaces of the terraces are undisrupted and these gently-dipping planar surfaces indicate that significant differential motion in the underlying basement cannot be accommodated. Finally, although abundant scattered talus blocks along terrace surfaces attest to the effectiveness of mass wasting processes in this environment, the relationships observed along our traverses suggest that even the mass wasting processes are now proceeding at a relatively slow rate. Talus blocks that litter the sea floor at the base of escarpments, or that are scattered across the surface of some terraces, are observed to be deeply inbedded in the surrounding sediment and there are no fresh scars, grooves or marks in the sediment surfaces proximal to outcrops to suggest the recent passage of a talus block. The well developed sedimented terraces, devoid of basement outcrops, and the exposure of semi-consolidated talus on steep escarpments, argue persuasively that mass wasting processes have been very effective in the past but, at present, the rate of mass wasting appears to have slowed and is characterized by infrequent events that are punctuated by relatively long periods of slope stability.

The apparent antiquity of the scarps and obvious effectiveness of mass wasting processes in the shaping of escarpment morphology makes it difficult to establish the structural fabric that initially created the outcrop geometry. The escarpments which expose consolidated debris have certainly been modified by erosion and it is not clear whether these exposures are originally the product of faulting with a dip-slip component of motion or whether these escarpments are largely constructional representing the steep front of an advancing wedge of debris shed from source terrain higher up the slope. As a first approximation, however, we have assumed that even if these escarpments of debris are constructional, their observed orientation should approximately mimic the overall strike of the source terrain. There is also an ambiguity about the original orientation of the bedrock-exposing escarpments because the morphologies of these bedrock exposures are largely controlled by the interplay between a spatially variable system of joints and slope decay. As a consequence, important structural information has long since been lost and it is not surprising that slickensides or other indicators of fault motion are not observed. Given these ambiguities, detailed structural analyses are precluded but a rose diagram of the orientation of all the escarpments observed on the north and south walls have been compiled and the strongest structural signal recognized is approximately parallel to the regional bathymetric contours (Figure 2). At the very least, faults must have originally been responsible for the creation of the scarps exposing plutonic and ultramafic rocks and these faults must have accommodated at least a component of dip-slip motion to create the observed relief. Although hard to detect in the face of the slope modifications caused by mass wasting, there is no evidence to suggest a component of strike-slip relative motion on these faults (i.e., rock promontories and intervening gullies that strike at a high angle to the trend of the transform are not offset).

Observations made during Dives 1019 (north wall) and 1018 (south wall) show that near the crest of the transform walls the topographic gradients decrease markedly (Figures 5b, 6). At a depth of approximately 2400 m on the north wall the sea floor gradients become very gentle (<5°) and an unbroken blanket of sediment dominates the seascape. During Dive 1019, after traversing a few hundred meters of this monotonous terrain, with no targets indentified on the sonar system, the submersible turned back to the south to investigate escarpments lower on the transform wall. On Dive 1018, at depths less than 2000 m, the bedrock-exposing escarpments of the south wall give way to steep slopes of consolidated talus which in turn give way to broad carbonate covered platforms that are ribbed by N–S trending ridges. These ridges are only about 10 m high with slopes that dip gently (10°) to the east and west and are covered with a semi-consolidated admixture of carbonate and Mn-encrusted rock. The rock fragments have a characteristic semi-circular shape in profile and exhibit a distinctive radial parting. These properties are diagnostic of rubble produced by the fragmentation of pillow lavas and we suggest that these N–S ridges are volcanic ridges that have essentially weathered in place and are mantled by a basalt-carbonate breccia. The advanced state of consolidation makes it difficult to sample this terrain but one sample of basalt (Dive 1018, Sta. 8) from such a locality supports this interpretation.

During the three ALVIN traverses up the north and south walls of the transform semi-consolidated carbonates as well as basaltic, plutonic, and ultramafic rocks were recovered from outcrops. The semi-consolidated carbonates were exclusively recovered from outcrops along the north wall. These rocks are composed of a mixture of very poorly preserved nannofossils that have been broken, dissolved or overgrown, and that are set in a matrix of recrystallized carbonate. The preservation of some discoasters permit the identification of *Ceratolithus actus* in two chalks (1019–5, 1019–13) suggesting that these rocks could be as old as lowermost Pliocene. A third chalk contained discoasters of the genus *Amaurolithus* indicating a faunal assemblage of uppermost Miocene age. The chalks were all burrowed and the fillings contain Late Pleistocene assemblages (M. Aubry, pers. communication).

Samples of basalts were recovered from accumulations of talus at four localities along the south wall of the transform and from one outcrop at the crest of the south wall during Dive 1018. The samples are vesicular with phenocrysts of plagioclase and olivine set in a microcrystalline groundmass composed mainly of clinopyroxene and plagioclase with lesser iron ores. The samples are devoid of fresh glass but all mineral phases are clear and unaltered with the exception of olivine which is often surrounded by iddingsite. In terms of petrography, these basaltic rocks are similar to basalts recovered by dredging from localities along the south wall of the OT (Shibata and Fox, 1975).

A suite of 12 plutonic rocks were recovered from 10 localities along the southern wall during Dives 1017 and 1018. These plutonic rocks are divisible, on the basis of mineral chemistry, whole rock chemistry and petrography into two major groups (OTTER, in prep.). The first group consists of two-pyroxene ferrogabbros in which the dominant minerals are orthopyroxene, clinopyroxene, plagioclase (An 39-18), magnetite and ilmenite. Additionally, two samples contain minor olivine. Accessory phases are apatite, hornblende, biotite, quartz and zircon (rarely). Although cumulate textures are not observed within this group of samples, whole-rock abundances of Zr (<90 ppm) and other incompatible trace elements indicate that these rocks are clearly accumulative in origin. These accumulative rocks, because of their highly differentiated mineral compositions, are interpreted to have formed by the crystallization of ferrobasaltic to quartz dioritic liquids.

The other group of plutonic rocks are diorites and quartz diorites, in which the dominant minerals are orthopyroxene, clinopyroxene, plagioclase (An 39-18), magnetite, ilmenite, amphibole, quartz, apatite and zircon. These rocks are all fine-grained and holocrystalline. Texturally, these rocks are aphyric and do not appear to be accumulative. Their high silica (52.3 to 64.7 wt.%) and Zr (200 to 650 ppm) contents suggest that, unlike the two-pyroxene gabbros noted above, these rocks appear to be the crystalline equivalent of liquid compositions. The present data suggests that diorite and quartz-diorite liquids, similar in composition to these holocrystalline rocks, represent the types of magmas from which the two-pyroxene gabbros noted above have formed by crystallization and accumulation.

Ultramafic rocks were collected at eight localities along the north wall and at four localities along the south wall. Harzburgites and lherzolites outcrop on both the north and south walls and all samples have been variably serpentinized exhibiting tectonite textures. The lherzolites are characterized by relic olivine, orthopyroxene, clinopyroxene and spinel grains set in a matrix of foliated serpentine minerals and secondary magnetite. The harzburgites are composed of large relic grains of orthopyroxene and minor spinel set in a matrix of serpentinite minerals and secondary magnetite. Many of the samples exhibit a well defined foliation and have been highly tectonized with pyroxene crystals deformed, fractured and recrystallized.

## 4. Discussion: A Geologic Model of the Transform Valley

During the last several million years the time averaged opening rate for the ridge axes north and south of the OT, as constrained by the age of diagnostic magnetic anomalies, is approximately 23 mm/yr$^{-1}$ (Fox *et al.*, 1969; Pitman and Talwani, 1972; Le Douaran *et al.*, 1982). The orientation of the slip-vector for North America/Africa in this area is not uniquely constrained but first motion studies of well determined earthquakes along the OT (Sykes, 1967; Udias *et al.*, 1976), solutions to the fit of magnetic anomaly pairs in the FAMOUS area to the north (Macdonald, 1977), a global synthesis of plate kinematic data (Minster and Jordan, 1978), as well as the orientation of the morphotectonic grain of the

Oceanographer Transform indicate that the slip-vector should have an E–W to WNW–ESE orientation.

This regional kinematic prespective provides important information about the first-order tectonic framework of this large-offset slowly-slipping transform but does not identify the individual tectonic elements within and along the transform domain and does not resolve how these tectonic components integrate spatially and temporally to create the first-order morphotectonic fabric of the transform boundary. The relief from the axis of the OT to the crest of the valley walls is greater than 2000 m, the regional gradients of the walls are 10° to 20°, and the cross-strike width of the valley is approximately 20 km. It is not clear from a regional kinematic perspective where the slip is located, how the slip is manifest at shallow levels, and what structures are responsible for the distinctive morphotectonic fabric of the transform domain. Approximately 100 km of submersible and deep-towed camera data provide new constraints on the fine-scale structure of the OT and document that two contrasting structural environments characterize the transform valley. Lying along the axis of maximum depth is an apparently braided network of recent fault scarps that disrupt the smooth sediment interface and that represents the plate boundary. This axial swath of on going tectonism is narrow and is flanked by the tectonically passive transform valley walls that have a staircase-like profile and that exhibit no evidence suggestive of recent faulting.

### 4.1. The Axis of Maximum Depth: The Transform Fault Zone

The intervals of recent scarp development across the transform valley floor create narrow (a few tens of meters to a few hundreds of meters wide) strands of tectonized sediment and these intervals are characterized by one or more of the following: abrupt changes of relief on the scale of meters to several meters, disruption of the sediment surface by the development of near vertical scarps (often closely spaced with relief of a meter or less) and steep slopes exhibiting evidence of recent and on going erosion (Figure 4). These structures integrate spatially to produce an anastomosing network of discontinuous strands of recent deformation (Figures 2, 8) that we interpret to represent the surficial expression of the slip that is taking place between the North American and African plates along this transform constituting a belt of neotectonism within the transform domain. We term this tectonic environment, following the terminology introduced by Tchalenko and Ambraseys (1970) and ARCYANA (1975), the transform fault zone (TFZ). Along the 25 km long segment of the transform that we investigated, the TFZ appears to be less than 4 km wide and centered around the axis of maximum depth.

All of the observed fault traces within the TFZ cut carbonate-rich, semi-consolidated ooze, accommodate at least a component of vertical motion creating relief of less than 1 meter, and must be relatively recent in origin because the fault-generated scarps are not easily preserved in the face of biodegradation and mass wasting. Although all the fault traces are relatively recent, a range of ages is

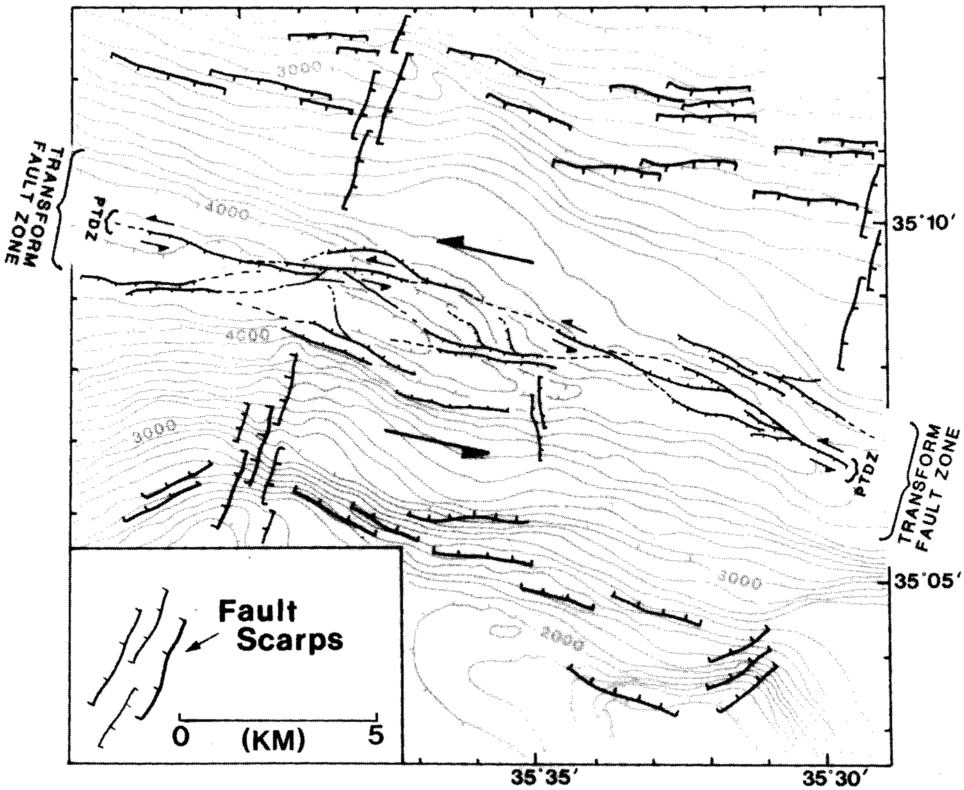


Fig. 8. A predictive model of the structural geometry that characterizes the central portion of the transform valley of the Oceanographer Transform. The majority of the strike-slip motion is taken up along and within a narrow belt (<4 km) of terrain that is centered around the axis of maximum depth and that is cut by a braided network of short, recently active fault strands of variable age and orientation – the transform fault zone (TFZ). The geometry within the TFZ is likely to be complex and continually evolving but, at any given time, it is likely that most of the slip will be taken up on a small number of faults that link along-strike to form a through-going strand – the principal transform displacement zone (PTDZ – Tchalenko and Ambraseys, 1970; ARCYANA, 1975). In response to changes in the rheology of rock bodies distributed along the transform, the development of asperities along the fault strands, and changes in relative plate motion, the location of the TFZ may migrate in time and space creating a swath of tectonized terrain.

suggested because some fault traces are sharp and angular in appearance whereas others have been badly modified by degradation. The limitations of our data precludes the definition of how these fault traces of different ages spatially interrelate. In the absence of definitive kinematic constraints for our field area, we use the fine-scale structural relationships documented to be characteristic of continental shear zones (e.g., Warne, 1955; Kingma, 1958; Skempton, 1966; Tchalenko and Ambraseys, 1970) as well as the structural geometry documented for the TFZ in Transform A (Choukroune *et al.*, 1978) as viable analogues for the kinematics of the TFZ in the Oceanographer. Based on these results, we suggest that one of the strands of deformed terrain within the portion of the TFZ investigated is likely to be through-going and represents a single narrow fault zone no more than a few hundred meters wide along which the major part of the present day ground movements are concentrated (Figure 8). This particular interval of most recent tectonism would represent the principal transform displacement zone (PTDZ). The state of stress within continental shear zones is known to be highly variable both spatially and temporally (e.g., Tchalenko and Ambraseys, 1970) and, as a consequence, the location of the PTDZ and the along-strike and across-strike geometry of the shear zones that comprise the PTDZ are not fixed in time. Although the actual geometry and kinematic history of the deformed strands of various ages within the TFZ of the Oceanographer cannot be resolved until more high-resolution data at a regional scale are obtained (i.e., deep-towed side-scan sonar data), we suggest that these multiple strands that comprise the TFZ reflect the complex and evolving state of strain that characterizes the transform interface.

It is notable that the fault strands do not expose one outcrop of basement or talus along or across the TFZ. The TFZ in the area studied lies along the axis of maximum depth and, therefore, is located along a linear depositional zone for debris shed from the high terrain of the flanking valley walls. This debris must have two primary components – an inorganic component representing debris shed from exposures of basement and a biogenic component largely composed of pelagic carbonate that rains down on this part of the North Atlantic sea floor at rates of 10 to 20 m per million years. In the area studied, the age of the seafloor on either side of the transform is approximately 5 my and the terrain at the plate edges has been evolving for this period of time indicating that by this age in the evolution of the transform enough debris has been deposited along the axis to cover essentially all of the original basement relief. Our data provides little information about the thickness of this sedimentary fill but 3.5 kHz records indicate that the sedimentary blanket is nearly continuous along the transform axis and that thicknesses are at least several tens of meters (Keith *et al.*, in prep.). Single channel seismic reflection profile data, although hard to interpret because of the strong and obscuring side echoes, suggest sedimentary thicknesses in some areas in excess of 100 m (Schroeder, 1977; Fox *et al.*, in prep.). The surprising lack of talus on the sea bed or on exposed scarps along this portion of the TFZ support the notion that the most recent (last million years) depositional phase along the TFZ has been dominated by the accumulation of carbonate and that talus shed from distal outcrops up on the transform walls is trapped on the broad sedimented lower slopes of the transform valley walls that flank the axis of maximum depth. Given the apparent high rates (tens of meters per million years) of sediment accumulation along the axis of the transform valley and the unstable nature of the semi-consolidated sedimentary fill, it is not surprising that only the most recent evidence for tectonism is observed. It is difficult for an older time-integrated structural fabric to develop in the sedimentary overburden because rates of slope decay (slope collapse) are relatively fast relative to the rates of slope generation (faulting).

None of the fault traces that comprise the TFZ exhibit geometric relationships that unequivocally document a component of strike-slip motion. In fact, some fault traces could not have accommodated a significant strike-slip component of motion because these faults define sinuous and undeformed traces. Several of the neotectonic zones, however, are characterized by sharply defined and straight scarp faces (Figure 4b, c, f) that, in the absence of definitive strain markers to the contrary, could have accommodated a strike-slip component of motion. At several localities, a cluster of mutually parallel scarps occur together in a closely-spaced (several meters to a few tens of meters) assemblage creating a distinctly pronounced lineated grain to the seafloor (Figure 4b, c) suggestive of a fabric that could be the product of strike-slip faulting.

The majority of the structures within the TFZ have orientations that are sub-parallel to the overall strike of the transform (090°–100°) or ±30° oblique to this trend. There is a secondary orientation maximum of structures between 150° and 160°. Given the ambiguities (i.e., difficult to rigorously fix the fault trace orientation; rapid slope decay obscures important structural details) inherent in interpreting these deep-towed photographic data, detailed structural interpretations are not warranted. This caveat not withstanding, the first motion solutions of earthquakes along this transform persuasively argues that left lateral strike-slip motion must be accommodated along this plate boundary (Sykes, 1967; Udias *et al.*, 1976) and it is instructive to interpret these fault-scarp orientation data in the light of what is known about the deformation of material in large, well-studied continental shear zones (i.e., Tchalenko and Ambraseys, 1970; Wilcox *et al.*, 1973).

As a first approximation, we assume that simple shear deformation, oriented at 100°, with a left-lateral component of relative motion is the cause of the fault pattern recognized within the TFZ of the Oceanographer at this locality. The structural analysis of faults produced in semi-consolidated sediments along presently active continental strike-slip fault zones (Tchalenko and Ambraseys, 1970; Wilcox *et al.*, 1973) indicate that strike-slip motion is accommodated by the development of shears with different but characteristic orientations (Cloos, 1928; Riedel, 1929; Tchalenko, 1970). Typically, shears form that are oriented 10° to 20° to the shear direction with the acute angle pointing along the relative movement ($R$ shears) and shears form that are inclined at a steep angle (60° to 70°) to the direction of movement ($R'$ shears). In kinematic terms, $R$ and $R'$ zones of shear cannot sustain large displacements parallel to the direction of shearing and strain is accommodated by the formation of crosscutting shears ($P$ shears) that are oriented in a direction approximately opposite to the $R$ shears. For sustained strain the $R$ and $P$ shears link up and significant strike-slip displacements are accommodated. The majority of the fault scarps that we define along the TFZ have orientations subparallel (±30°) to the assumed regional slip vector for this portion of the OT and could, therefore, represent traces of $R$ and $P$ shears. The fault traces with orientations of 150° to 160° may reflect compressional structures that formed either as a result of simple shear or as a result of local stresses due to the along-strike linking of $R$ and $P$ shears.

We suggest that the location of the TFZ along the axis of maximum depth is not fortuitous but a direct consequence of the rheology of a large-offset slowly-slipping RTR plate boundary (Fox and Gallo, 1984). Our field experiment straddles the center of the OT and, given the 120 km offset of the plate boundary and the spreading rate for this area (12 mm yr$^{-1}$ half rate), the transform juxtaposes lithosphere that is approximately 5 my old. For oceanic lithosphere of this age the thickness of the lithosphere should be approximately 20 km thick (e.g., Parker and Oldenburg, 1973) and the strains associated with strike-slip tectonism will be focused along a relatively narrow crush zone located at the edges of the opposing plates.

### 4.2. The transform valley walls

The inward facing walls of the OT exhibit regional slopes of 20° and create relief ranging from 2000 to 3000 m. This relief is clearly not the product of dip-slip motion on a few large throw faults, but rather the integration of the relief generated on a large number of small throw faults with a relatively small component of dip-slip motion (< 100 m, Figure 9). From those scarps sampled along the north wall ultramafic rocks and semi-consolidated carbonate, some of which is Miocene in age, are routinely sampled. Along the south wall escarpments, gabbros and diorites are the only rock type recovered *in situ* but ultramafic, gabbroic and, to a lesser extent, basaltic rocks are all recovered from exposures of talus. The fault scarps are oriented parallel to the regional morphotectonic trends defined by surface ship bathymetry. Terraces of variable width separate the fault traces giving the transform valley walls a distinctive staircase-like architecture in profile with the opposing edges of oceanic lithosphere stepping down towards the TFZ. Debris generated by erosion of material exposed on faults traces along with remobilized carbonate is shed from high terrain producing debris fans that cover small-relief scarps and flat-lying bedrock creating sedimented terraces (Figure 9). At the lower levels of the transform valley the accumulation of sediments has been so substantial that broad, continuous and monotonous sedimented slopes dominate the seascape. The sediments that blanket much of the transform valley slopes are an effective strain marker and our *in situ* data document that these sedimented surfaces are smooth and undisrupted indicating that there is little recent differential motion between the fault bounded blocks that step the lithosphere down to the axis of maximum depth.

These field relationships that characterize the central portion of the OT place important constraints on our understanding of the shallow-level crustal structure of the transform walls and of the processes that shape the morphotectonic character of the transform walls. We interpret the routine recovery of gabbroic, ultramafic and dioritic rocks on small throw faults located high up on the walls of the transform valley to indicate that the oceanic crust must be thin and, in places,

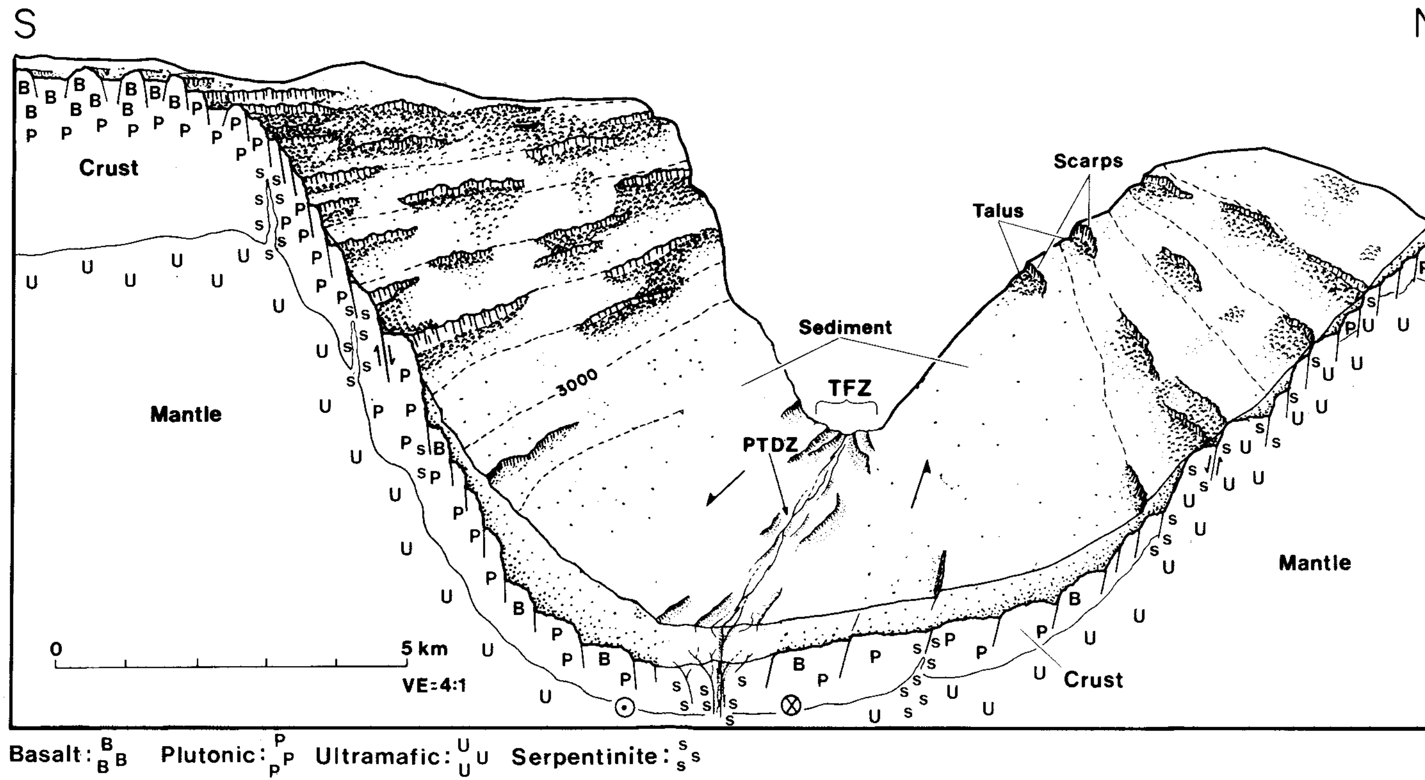


Fig. 9. A schematic three-dimensional view of a section of the OFZ transform valley. The vertical exaggeration is approximately 4 : 1. Strike-slip deformation along the transform valley is reflected by the transform fault zone (TFZ); the majority of strike-slip displacement at a given time is confined to the principal transform displacement zone (PTDZ). The thickness of the oceanic crust is inferred from the observed distribution of rock-types. Whereas the lower portions of the transform valley walls are characterized by undisrupted sediment, at higher elevations numerous scarps expose a diverse assemblage of mostly plutonic and ultramafic rocks. See text for discussion.

discontinuous. Our sampling density is not sufficiently large to elucidate details but a few clues as to the distribution of crustal lithologies emerge and are worth mentioning. The traverse up the north wall of the transform valley (Dive 1019) recovered only partially serpentinized ultramafic rocks at outcrops and from accumulations of talus. This rather monotonous distribution of rock over a distance of 2500 m suggests that in this area a basaltic crust comprised of basalt and gabbro is largely absent. In contrast, along the two traverses up the south wall (Dives 1017, 1018) plutonic rock, with varied compositions, textures, metamorphic effects and strain histories, was the only rock type recovered *in situ* but the range of rock types recovered from talus is very diverse (basaltic, gabbroic and ultramafic rocks) indicating that the distribution of rocks in this area is very heterogenous. Although rigorous sampling programs must be implemented to define the vertical and lateral distribution of major rock types across and along transform valleys, it seems clear from this exploratory investigation that this tectonic environment is characterized by a complex arrangement of igneous units that vary at a scale of hundreds of meters to a few thousand meters. The contact between units are likely to be steeply dipping and defined by faults or by an intrusive interface caused by the diapiric rise of serpentinite.

These sampling results support the prediction, based on a compilation of dredging results, of Francheteau *et al.* (1976) that the crust associated with slowly-slipping RTR plate boundaries is likely to be anomalous in terms of crustal thickness. This apparent thin crustal assemblage must be a characteristic created during or shortly after the creation of oceanic lithosphere because *in situ* sampling of young oceanic lithosphere (<1.5 my) by submersible ALVIN at or proximal to three slowly-slipping ridge-transform intersections (Mid Cayman Rise-CAYTROUGH, 1979; Stroup and Fox, 1981; Kane Transform-Karson and Dick, 1983; and Oceanographer Transform-OTTER, 1984), show that a varied assemblage of gabbroic and/or ultramafic rocks are frequently recovered from small throw, dip-slip faults that occur along the walls of the rift valley. These investigators conclude that the oceanic crust created at this type of plate boundary is anomalously thin (<1 km) and that this thin assemblage of basalts and gabbros is subsequently disrupted and dismembered by faulting and mass wasting on the walls of the rift valley. The crustal structure is further complicated when faults penetrate the thin crustal carapace creating permeable pathways along which water travels hydrating the underlying upper mantle rocks. Serpentinized bodies then rise diapirically through the thin crust mixing altered upper mantle rocks with crustal components along steep intrusive contacts. This model for heterogeneous crustal structure created at slowly slipping ridge-transform intersections predicts that a similar complex crustal structure should be observed along the transform valley walls of a slowly slipping transform (Figure 9).

The oceanic lithosphere exposed on the opposing transform valley walls investigated during our exploration of the OT is about the same age. Therefore, the morphologic relationships documented along the walls investigated will be the integrated product of a range of processes (e.g., faulting, mass wasting, volcanism, diapirism) that have operated in space and time since the creation of these portions of the plate boundary 5 my ago. The badly degraded rock scarps, and the existence of wide sedimented terraces attest to the effectiveness of mass wasting during the earlier history of this terrain. There is no evidence for recent faulting along the existing bedrock exposures or across the sedimented terraces suggesting that there is little or no differential motion between blocks along the walls. It is apparent that even the processes of slope decay and modification was not as vigorous today as in the past because there are no expressions of recent slope decay (i.e., fresh talus, skid markings in sediment). The scarps that expose bedrock must have been originally created by faulting that accommodated at least a component of dip-slip motion. Whether or not these faults ever accommodated significant amounts of strike-slip motion cannot be established from our data but we suspect, following the results of Karson and Dick (1983) and OTTER (1984), that little differential strike-slip motion has been accommodated on these scarps.

Given these relationships, we propose that the great relief and distinctive morphology of the transform walls have little to do with the strike-slip faulting that is the tectonic signature of transform faults. Rather, the rapid increase in depth of the sea floor as the transform boundary is approached, creating the transform valley walls, reflects profound changes in the properties of the underlying lithosphere caused by the juxtaposition of a thick edge of lithosphere against an accreting plate boundary at a ridge-transform intersection (Fox and Gallo, 1984). Over distances of 10 to 20 km, as the transform boundary is approached, the magmatic budget will diminish continuously because melt generation processes in the rising wedge of asthenosphere will be attenuated by lower temperatures, higher viscosities and perturbations in flow. In turn, these effects will lead to the emplacement of a thin crust and a heterogeneous upper mantle comprised of undepleted and depleted peridotites as well as trapped basaltic melt. The increase in depth of the sea floor towards the transform boundary reflects an isostatic response of the lithosphere to a thinned crust, a marked change in mass distribution in the upper mantle, and an overall thickening of the lithosphere. Our data suggests that this isostatically driven deepening of the oceanic lithosphere proximal to the OT is accommodated by the development of numerous dip-slip faults that step the sea floor down to the transform boundary. These faults are generated when the lithosphere is young (<2 my; Karson and Dick, 1983; OTTER, 1984) and, after generation, these faults accommodate little differential motion except local uplift caused by the diapiric rise of hydrated upper mantle rocks and subsidence associated with lithospheric aging (DeLong *et al.*, 1979).

The model outlined above is largely based on the *in situ* sampling results made by submersible ALVIN at a number of localities in or proximal to RTR plate boundaries (CAYTROUGH, 1978; Stroup and Fox, 1981; Karson and Dick, 1983; OTTER, 1984), that establish profound small-scale heterogeneity and compositional variability of the rock types composing the fracture zone environment. These results cannot be considered anomalous because carefully constrained seismic refraction experiments have also been carried in the last several years along fracture zones and show that velocity structure of RTR plate boundaries at a regional scale is anomalous (Detrick and Purdy, 1980; White and Mathews, 1980; Detrick *et al.*, 1982; Sinha and Louden, 1983; Cormier *et al.*, 1984). These results document that the seismically determined crustal structure of several slowly slipping fracture zones is anomalous when compared to normal oceanic crust with crustal structure varying markedly both along and across strike. Of particular interest are the results of a refraction experiment carried out in an around the Oceanographer Fracture Zone (Sinha and Louden, 1983). These results show that the axis of the fracture zone is characterized by crust that is typically only 3–4 km thick with thickness ranging between 1 and 5 km. At shallow crustal levels along the fracture zone valley the crustal velocities are low and the velocity gradients are very steep indicative of increased porosity due to fracturing. Furthermore, some degree of crustal thinning is recognized as the fracture zone is approached. These seismic refraction results, which determine the velocity structure of the crust on a scale of thousands of meters, establish that the compositional and structural complexities occurring on a small scale integrate in a non-systematic way to create an anomalous and variable velocity structure.

The seismically-constrained crustal velocity structure for the slowly slipping OT, however, cannot be easily translated into a geologic model for a number of reasons: a wide range of igneous and metamorphic rocks are known to be exposed on the walls of the OT (Fox *et al.*, 1976; this study); these rock types are distributed at scales generally much less than the seismic scale; the laboratory determined velocities of representative samples recovered from the OT indicate that, under appropriate confining pressures, a diverse range of rock types can satisfy a given crustal velocity interval (Fox *et al.*, 1976); and the contacts between rock bodies, caused by intrusion or faulting, are likely to be steep. Therefore, the seismically determined velocity structure represents an averaging of these documented small-scale heterogeneities. Moreover, the geologic significance of seismically determined thin crust cannot be uniquely determined because any one of three significantly different geologic environments could be responsible for the development of seismic Moho. The seismic boundary between mantle velocities ($>8.0\ \mathrm{km\ sec^{-1}}$) and crustal velocities ($<7.5\ \mathrm{km\ sec^{-1}}$) could signify the contact between an overlying cumulate magnetic sequence, dominated by cumulate gabbros and lesser amounts of cumulate ultramafics, with the underlying residual ultramafic rocks (tectonized harzburgites) from which the overlying magmatic sequence was extracted (Fox *et al.*, 1973; Christensen and Salisbury, 1975; Karson *et al.*, 1984). Second, instead of representing the boundary between magmatic and residual rocks, Moho could be defined by the transition within the basal cumulate sequence from gabbroic rocks downwards into a sequence of cumulate ultramafic rocks (e.g., dunite, pyroxenites; Casey *et al.*, 1981; Karson *et al.*, 1984). Third, Moho in and proximal to the fracture zone could represent the depth to which water has penetrated into ultramafic terrain and signify the contact between the overlying serpentinized rocks and the underlying unhydrated upper mantle (Fox *et al.*, 1976; Detrick *et al.*, 1983; Sinha and Louden, 1983). Indeed, all three contacts are likely to be developed proximal to slowly slipping RTR plate boundaries for a number of environmental reasons: smaller volumes of melt are likely to be produced proximal to the cold truncating edge of the transform creating a thin magmatic crust (Fox and Gallo, 1984; Bender *et al.*, 1984; Langmuir and Bender, 1984); greater degrees of fractionation may occur in small shallow level magma reservoirs creating thick sequences of cumulate ultramafic rocks (Karson and Dewey, 1978; Karson, 1984); and, finally, the thin or nonexistent crust allows water to penetrate into basal ultramafics creating a front of serpentinization (Fox *et al.*, 1976; Detrick *et al.*, 1983, Sinha and Louden, 1983).

## 5. Concluding Remarks

The geologic model outlined in Section 4 and shown in Figures 8 and 9 proposes that the distribution of rock bodies within the crust and upper mantle proximal to a slowly slipping RTR plate boundary is exceedingly complex and that the transform domain of a RTR plate boundary is composed of two tectonic environments. First, there is that relatively narrow portion of the transform domain that has been the locus of strike-slip tectonism. We suggest that for any given time interval the strike-slip zone will be characterized by a family of anastomosing fault strands (TFZ, Figures 8, 9). The TFZ is narrow (<4 km) and is centered along the axis of maximum depth. Instantaneously, it is likely that the TFZ may contain a single through-going strand along which most of the slip is concentrated (PTDZ; Figures 8, 9). Because of asperities in fault geometry, rheological differences in rock types, and changes in the pole of relative motion, we propose that the fault geometry of the TFZ will migrate in time and space creating a swath of tectonized terrain. The second tectonic environment is defined by the relatively broad flanks of transform domain that lie to each side of the TFZ creating the inward facing walls of the transform valley. Our data indicate that the several thousand meters of relief created by these walls are the integrated product of a large number of inward facing scarps that accommodate dip-slip motion and, apparently, accommodate little or no strike-slip motion (Figures 8, 9). A diverse range of plutonic and ultramafic rocks outcrop on these scarps suggesting that the crust is thin and/or discontinuous. We suggest that this complex igneous assemblage is the product of anomalous accretionary processes that are characteristic of slowly-slipping RTR plate boundaries (Fox *et al.*, 1980; Stroup and Fox, 1981; Sinha and Louden, 1983; Karson and Dick, 1983; Fox and Gallo, 1984; OTTER, 1984; White, 1984). The great relief associated with this portion of the transform domain reflects major changes in the distribution of mass within the upper portions of the lithosphere as the transform boundary is approached.

## Acknowledgements

The authors wish to thank the officers and crew of the R/V KNORR and R/V LULU and the members of the ALVIN submersible team for their help during the field program; without their assistance, dedication, and expertise this project would not have been possible. Grants from the Office of Naval Research supported the field work and the data analysis and is gratefully acknowledged; the following grants supported the program: N-0014-80-C-0287 (P.J.F., J.A.K., H.S., W.S.F.K., J.B.S., D.J.F., D.G.G.); N-00014-81-C-0820 (P.J.F., H.S., D.G.G.); N-00014-80-C-098-S.W. (K.C.); N-00014-80-C-0098-S.T. (E.B., P.H.). WHOI contribution number 5992.


## References


ARCYANA: 1975, 'Transform Fault and Rift Valley from Bathyscaphe and Driving Saucer', *Science* **190**, 108–116.

Bender, J. F., Langmuir, C. H., and Hanson, G. N.: 1984, 'Petrogenesis of Basalts from the Tamayo Region, East Pacific Rise: Correlation of Glass Chemistry with Distance from a Transform Fault', *Jour. Petrology* **25**, 213–254.

Casey, J. F., Dewey, J. F., Fox, P. J., Karson, J. A., and Rosencrantz, E.: 1981, 'Heterogeneous Nature of Oceanic Crust and Upper Mantle: A Perspective from the Bay of Islands Ophiolite Complex', in C. Emiliani (ed.), *The Sea, 7, The Oceanic Lithosphere*, John Wiley and Sons, N.Y., 305–338.

CAYTROUGH: 1979, 'Geological and Geophysical Investigations of the Mid-Cayman Spreading Center: Initial Results and Observations', in Talwani, M., Harrison, C. G., and Hayes, D. E. (eds.), *Deep Drilling Results in the Atlantic Ocean: Ocean Crust 2nd Maurice Ewing Memorial Symp.*, Amer. Geophys. Union, **2**, 66–93.

Choukroune, P., Francheteau, J., and LePichon, X: 1978, 'In Situ Structural Observations along Transform Fault A in the Famous Area, Mid-Atlantic Ridge', *Bull. Geol. Soc. Amer.* **89**, 1013–29.

Christensen, N. I. and Salisbury, M. H.: 1975, 'Structure and Constitution of the Lower Oceanic Crust', *Rev. Geophys. Space Physics* **13**, 57–86.

Cloos, H.: 1928, 'Experimente Zu Inneren Tektonik', *Centralbl. Mineral Geol. y. Pal.* **1928B**, 609–621.

Cormier, M. H., Detrick, R. S., and Purdy G. M.: 1984, 'Seismic Refraction Studies of the Kane Fracture Zone', *Jour. Geophys. Res.* **89**, 10,249–10,266.

DeLong, S. E., Dewey, J. F., and Fox, P. J.: 1979, 'Topographic and Geologic Evolution of Fracture Zones', *Jour. of Geol Soc. Lond.* **136**, 303–310.

Detrick, R. S. and Purdy, G. M.: 1980, 'The Crustal Structure of the Kane Fracture Zone from Seismic Refraction Studies', *Jour. Geophys. Res.* **85**, 3759–77.

Detrick, R. S., Mudie, J. D., Luyendyk, B. P., and Macdonald, K. C.: 1973, 'Near Bottom Observations of an Active Transform Fault (Mid-Atlantic Ridge at 37° N)', *Nature Phys. Sci.* **246**, 59–61.

Detrick, R. S., Cormier, M. M., Prince, R., and Forsyth, D. W.: 1982, 'Seismic Constraints on the Crustal Structure within the Vema Fracture Zone', *Jour. Geophys. Res.* **87**, 599–10,612.

Fox, P. J., Pitman, W. C. III, and Shepard, F.: 1969, 'Crustal Plates in the Central Atlantic: Evidence for at least Two Poles of Rotation', *Science* **165**, 487–489.

Fox, P. J., Schreiber, E., and Peterson, J. J.: 1973, 'The Geology of the Oceanic Crust: Compressional Wave Velocities of Oceanic Rocks', *Jour. Geophys. Res.* **78**, 5155–5172.

Fox, P. J., Schreiber E., Rowlett, H., and McCamy, K.: 1976, 'The Geology of the Oceanographer Fracture Zone: A Model for Fracture Zones', *Jour. Geophys. Res.* **81**, 4117–4128.

Fox, P. J., Detrick, R. S., and Purdy, G. M.: 1980, 'Evidence for Crustal Thinning Near Fracture Zones: Implications for Ophiolites', in Panayiotou, A. (ed.), *Proc. Int. Ophiolite Symp.*, Cyprus, Geol. Sur. Dept., Nicosia, 161–168.

Fox, P. J., Schroeder, F., Moody, R. H., and Pitman, W. C. III: 1986, 'The Morphotectonic Character of the Oceanographer Fracture Zone', *Marine Geophys. Res.* (in prep.)

Fox, P. J. and Gallo, D. G.: 1984, 'A Tectonic Model for Ridge-Transform-Ridge Plate Boundaries: Implications for the Structure of Oceanic Lithosphere', *Tectonophysics* **104**, 205–242.

Francheteau, J., Choukroune, P., Hekinian, R., Le Pichon, X., and Needham, D.: 1976, 'Oceanic Fracture Zones Do Not Provide Deep Sections into the Crust', *Can J. Earth Sci.* **13**, 1223–1235.

Heezen, B. C. and Tharp, M.: 1968, 'Physiographic Diagram of the North Atlantic (new edition)', Geol. Soc. Amer., New York, N.Y.

Heezen, B. C., Bunce, E. T., Hersey, J. B., and Tharp, M.: 1964a, 'Chain and Romanche Fracture Zones', *Deep Sea Research* **11**, 11–33.

Karson, J. A.: 1984, 'Variations in Structure and Petrology in the Coastal Complex, Newfoundland: The Anatomy of an Oceanic Fracture Zone', in I. G. Gass, S. J. Lepard, and A. W. Sheldon (eds.) *Ophiolites and Oceanic Lithosphere*, Blackwell Scientific, **13**, 131–144.

Karson, J. A. and Dewey, J. F.: 1978, 'Coastal Complex, Western Newfoundland: An Early Ordovician Oceanic Fracture Zone', *Bull. Geol. Soc. Amer.* **89**, 1037–1049.

Karson, J. and Dick, H. J. B.: 1983, 'Tectonics of Ridge-Transform-Intersections at the Kane Fracture Zone', *Mar. Geophys. Res.* **6**, 51–98.

Karson, J. A., Collins, J. A., and Casey, J. F.: 1984, 'Geologic and Seismic Velocity Structure of the Crust/Mantle Transition in the Bay of Island Ophiolite Complex', *Jour. Geophys. Res.* **89**, 6126–6138.

Keith, D., Fox, P. J., and Karson, J. A.: 1986, 'The Role of Mass Wasting and the Evolution of the Morphology of Slowly-Accreting Plate Boundaries', (in prep.)

Kingma, J. T.: 1958, 'Possible Origin of Piercement Structures, Local Unconformities, and Secondary Basins in the Eastern Geosyncline, New Zealand', *New Zealand Jour. Geology and Geophysics* **1**, 269–274.

Langmuir, C. H. and Bender, J. F.: 1984, 'Chemical Variations of ORB in the Vicinity of Transform Faults: Observations and Implications', *Earth Planet. Sci. Lett.* **69**, 107–127.

Le Douaran, S., Needham, H. D., and Francheteau, J.: 1982, 'Pattern of Opening Rates along the Axis of the Mid-Atlantic Ridge', *Nature* **300**, 254–257.

Macdonald, K. C.: 1977, 'Near-bottom Magnetic Anomalies, Asymmetric Spreading, Oblique Spreading, and Tectonics of the Mid-Atlantic Ridge near Lat. 37° N', *Geol. Soc. Am. Bull.* **88**, 541–555.

Macdonald, K. C. and Luyendyk, B. P.: 1977, 'Deep-tow Studies of the Structure of Mid-Atlantic Ridge Crest near 37° N (FAMOUS)', *Geol. Soc. Amer. Bull.* **88**, 621–636.

Minster, J. B. and Jordan, T. H.: 1978, 'Present-Day Plate Motions', *Jour. of Geophysical Res.* **83**, 5331–5354.

OTTER: 1984, 'The Geology of the Oceanographer Transform: The Ridge-Transform Intersection', *Marine Geophys. Res.* **6**, 109–41.

OTTER: 'The Petrology of Rocks Recovered from Outcrops along the Oceanographer Transform and Adjoining Rift Valley', (in prep.).

Parker, R. L. and Oldenberg, D. W.: 1973, 'Thermal Model of Ocean Ridges', *Nature Phys.* **242**, 137–139.

Phillips, J. D. and Fleming, M. S.: 1978, 'Multi-Beam Sonar Study of the Mid-Atlantic Rift Valley 36°–37° N FAMOUS', Geol. Soc. Amer., MC-19.

Pitman, W. C. III, and Talwani, M.: 1972, 'Seafloor Spreading in the North Atlantic', *Geol. Soc. America Bull.* **83**, 619–46.

Riedel, W.: 1929, 'Zur Mechanik Geologischer Brucherscheinungen', *Centralbl. Mineral Geol. U. Pal.* **1929B**, 354–368.

Schroeder, F. W.: 1977, 'A Geophysical Investigation of the Oceanographer Fracture Zone and the Mid-Atlantic Ridge in the Vicinity of 35° N', Ph.D. Thesis, Columbia University, 458 pp.

Shibata, T. and Fox, P. J.: 1975, 'Fractionation of Abyssal Tholeiites: Samples from the Oceanographer Fracture Zone (35° N, 35° W)', *Earth and Planet. Sci. Letters* **27**, 62–72.

Sinha, M. C. and Louden, K. E.: 1983, 'The Oceanographer Fracture Zone, 1. Crustal Structure from Seismic Refraction Studies', *J. R. Astr. Soc. London* **75**, 713–736.

Skempton, A. W.: 1966, 'Some Observations of Tectonic Shear Zones', *Proc. 1st. Cong. Internat. Soc. Rock. Mech., Lisbon* **1**, 329–335.

Stroup, J. B. and Fox, P. J.: 1981, 'Geologic Investigations in the Cayman Trough: Evidence for Thin Crust along the Mid-Cayman Rise', *Jour. Geophys. Res.* **75**, 2748–52.

Sykes, L. R.: 1967, 'Mechanism of Earthquakes and Nature of Faulting on the Mid-Oceanic Ridges', *Jour. Geophys. Res.* **72**, 2131–2153.

Tchalenko, J. S.: 1970, 'Similarities Between Shear Zones of Different Magnitudes', *Geol. Soc. Amer. Bull.* **81**, 1625–40.

Tchalenko, J. S. and Ambraseys, N. M.: 1970, 'Structural Analysis of the Dasht-e-Bayez (Iran) Earthquake Fractures', *Geol. Soc. Amer. Bull.* **81**, 41–60.

Udias, A., Lopez, A., and Mezcua, J.: 1976. 'Seismotectonics of the Azores – Alboran Region', *Tectonophysics* **31**, 259–289.

Warne, A. H.: 1955, 'Ground Fracture Patterns in the Southern San Joaquin Valley Resulting from the Arvin – Tehachapi Earthquake', *California Div. Mines and Geology Bull.* **171**, 57–66.

White, R. S.: 1984, 'Atlantic Oceanic Crust: Seismic Structure of a Slow Spreading Ridge', in I. G. Gass, S. J. Lepard, A. W. Shelton (eds.), *Ophiolites and Oceanic Lithosphere*, Geol. Soc. London Spec. Pub., 101–111.

White, R. S. and Matthews, D. H.: 1980, 'Variations in Oceanic Crustal Structure in a Small Area of the North-Eastern Atlantic', *Geophys. Jour. Roy. Soc.* **61**, 401–436.

Wilcox, R., Harding, T., and Sealy, D. R.: 1973, 'Basic Wrench Tectonics', *Amer. Assoc. Petrol. Geol. Bull.* **57**, 74–96.

Williams, C. A., Louden, K. E., and Tanner, S. J.: 1984, 'The Western Intersection of Oceanographer Fracture Zone with the Mid-Atlantic Ridge', *Marine Geophys. Res.* **6**, 143–58.

Wilson, J. T.: 1965, 'New Class of Faults and their Bearing on Continental Drift', *Nature* **207**, 343–347.